ORIGINAL PAPER

Can Satraplatin be hydrated before the reduction process occurs? The DFT computational study

**Ondřej Bradáč · Tomáš Zimmermann ·
Jaroslav V. Burda**

Abstract Hydration reactions of two anticancer Pt(IV) complexes JM149 and JM216 (Satraplatin) were studied computationally together with the hydration of the Pt(II) complex JM118, which is a product of the Satraplatin reduction. Thermodynamic and kinetic parameters of the reactions were determined at the B3LYP/6-311++G(2df.2pd)// B3LYP/6-31 + G(d)) level of theory. The water solution was modeled using the COSMO implicit solvation model, with cavities constructed using Klamt's atomic radii. It was found that hydration of the Pt(IV) complexes is an endergonic/ endothermic reaction. It follows the (pseudo)associative mechanism is substantially slower ($k \approx 10^{-11}$ s^{-1}) than the corresponding reaction of Pt(II) analogues (($k \approx 10^{-5}$ s^{-1}). Such a low value of the reaction constant signifies that the hydration of JM149 and Satraplatin is with high probability a kinetically forbidden reaction. Similarly to JM149 and Satraplatin, the hydration of JM118 is an endothermic/endoergic reaction. On the other hand, the kinetic parameters are similar to those of cisplatin Zimmermann et al. (J Mol Model 17:2385–2393, 2011), allowing the hydration reaction to occur at physiological conditions. These results suggest that in order to become active Satraplatin has to be first reduced to JM118, which may be subsequently hydrated to yield the active species.

Keywords Platinum metallodrugs · Computational study · DFT · Thermodynamics · Rate constants

O. Bradáč · T. Zimmermann · J. V. Burda (✉)
Department of Chemical Physics and Optics,
Faculty of Mathematics and Physics, Charles University,
Ke Karlovu 3,
121 16 Prague 2, Czech Republic
e-mail: burda@karlov.mff.cuni.cz

Introduction

In this study, the hydration of the new platinum compounds is explored and compared to hydration reactions of cytostatic analogues of cisplatin. The Pt(II) complexes are treated for more than three decades in chemotherapy of malign tumors [2–4]. The details of the mechanism of anticancer activity of the platinum complexes may be found in many studies, e.g., see refs. [5]. General issue common to the drugs used in anticancer therapy is the resistance of tumor cells (both intrinsic and acquired after several administrations). Cisplatin is no exception in this respect. To overcome the resistance, cisplatin is usually administered in various cocktails where several cytostatics are mixed for more selective effect. Another strategy to overcome the resistance is the development of new agents, which are often derived from the active parent compound. In the framework of these efforts, many cisplatin analogs were discovered with similar antitumor activity and lower resistance in comparison with cisplatin. Famous examples are, e.g., carboplatin or oxaliplatin, which both successfully passed the clinical tests [3]. They are square-planar complexes with central Pt(II) cation and ligands in the cis configuration, similarly to the parent compound cisplatin (cis-Pt[$Cl_2(NH_3)_2$]). Lately, other cis square planar complexes appeared with ammine groups replaced by heterocyclic ligands [6]. Interestingly - despite the generally accepted assumption of structure-activity (function) relationship - it was also found that some derivatives of the inactive complex transplatin also exhibit anticancer activity [7–9].

Besides extensive experimental work devoted to study of the Pt(II) anticancer compounds many computational models try to complement experimental results with a deeper understanding of reaction mechanisms. The most relevant in relation to this subject are studies done by

Deubel [10, 11], Chval [12, 13], Eriksson [14, 15], Dos Santos [16–22] or Carloni [23, 24]. Several ab initio and DFT studies on platinum(II) reactivity were published also by our laboratory, including works on the hydration process [1, 25, 26], the interactions with nucleobases [27–30] or the interactions with the amino acids [31–33].

Very interesting and promising properties were discovered in another class of platinum complexes, which contains central Pt(IV) cation. The most successful representative of this class is complex JM216 (trans-bis(acetato)ammine-cis-dichloro(cyclohexylamine)Pt(IV)) [34, 35]. This complex, named in clinical practice as Satraplatin, is currently in the third phase of clinical tests [36]. Satraplatin is one of the first Pt-metallodrugs that can be administered orally. Several analogs of Satraplatin, e.g., JM149 (ammine-cis-dichloro-(cyclohexylamine)-trans-dihydroxo platinum (IV)) are also active and were examined by Goddard [37]. Both JM216 and JM149 are depicted in Scheme 1.

Main motivation for this study stems from discussions in the literature where different opinions exist on the metabolism and reaction mechanisms of these complexes [38–41]. The most crucial question is whether the Satraplatin complex a) hydrates before the Pt(IV) drug is reduced to Pt(II) complex as shown in Scheme 2 [40], or b) is reduced first and later hydrated, i. e. it is first reduced to JM118 [34], which further exchanges its chloro ligands by aqua ligands.

In the sake of comparison, JM149 complex was considered too, applying the same reaction mechanism. Complete thermodynamic and kinetic description is presented in this work.

Computational details

The hydration reaction, which is assumed as the chloro-ligand replacement by the water molecule, is studied in the supermolecular approach with both interacting particles considered as a single weakly bonded system. All compounds involved in the hydration reactions of JM149, JM216, and JM118 as reactants, transition states or products were optimized using the density functional theory (DFT) with the B3LYP functional and the 6-31+G(d) basis set. The reactions were studied in the gas phase and in the aqueous solution, which was simulated by the COSMO model [42, 43]. Platinum and chlorine atoms were described by the quasirelativistic Stuttgart effective core potentials (Pt: MWB-60 [44] and Cl: MWB-10 [45]). The original set of pseudoorbitals was augmented by a set of the appropriate diffuse and polarization functions (α_s(Pt)=0.0075, α_p(Pt)= 0.013, α_d(Pt)=0.025, α_f(Pt)=0.998, and α_d(Cl)=0.618 as discussed in ref. [25], diffuse α_s(Cl) and α_p(Cl) were taken from the Pople's 6-31+G basis set [46]). This basis set is
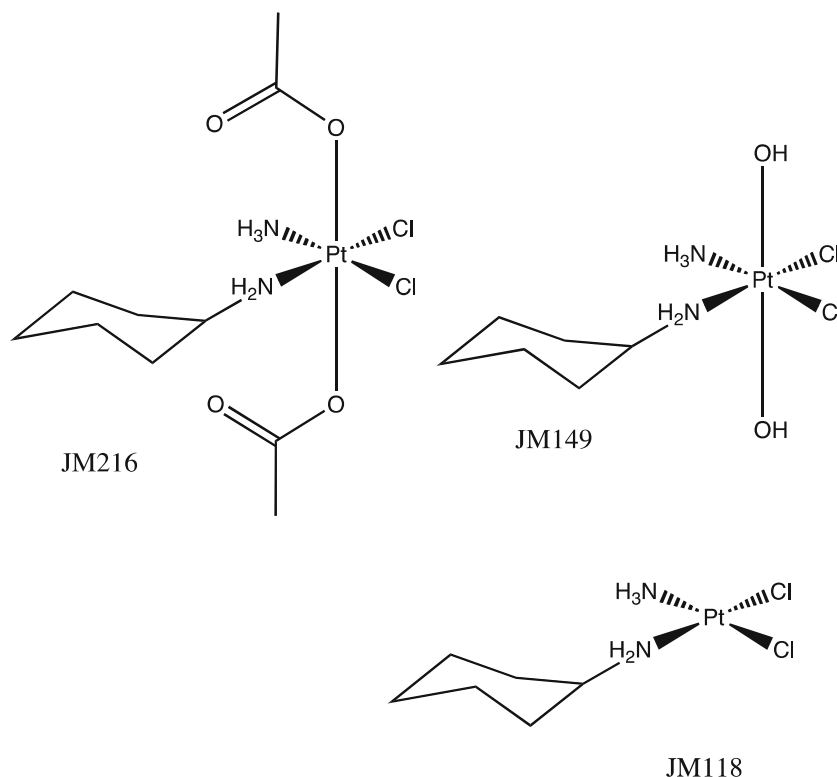
Scheme 1 Isolated reactant complexes explored in the study

JM216   JM518   JM559   JM383 (metabolite B)

reduction

JM118 (metabolite E)
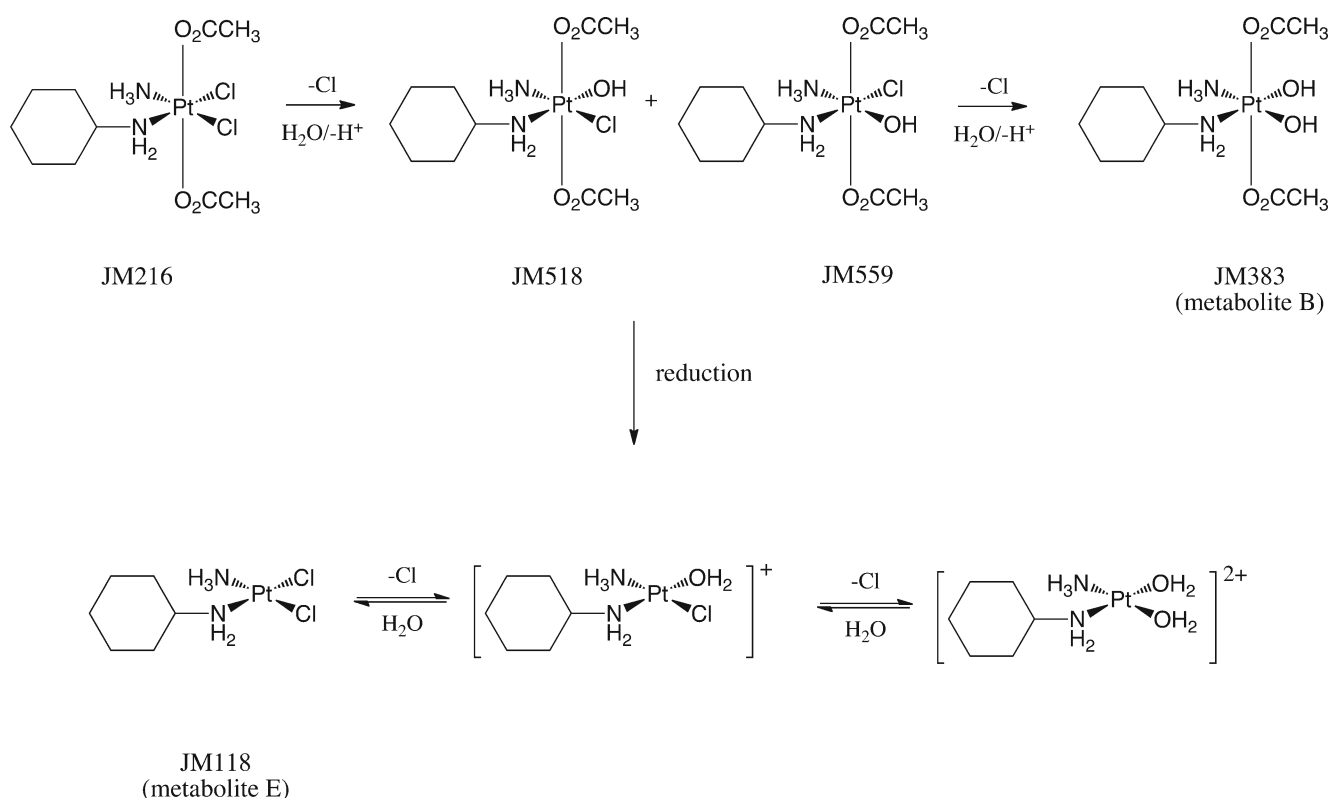
Scheme 2 Reaction mechanism adapted from Raynaud et al. [40]

labeled BSop hereinafter. The frequency analysis was performed at the same level of theory, confirming the appropriate character of all the stationary points. In the case of transition state structures, a single negative eigenvalue of the Hessian matrix corresponds to the appropriate antisymmetric stretching vibration mode. The single-point (SP) electronic energies of the optimized structures from the hydration reaction profile were determined with the augmented triple-zeta basis set 6-311++G(2df,2pd) with a consistent extension of the Pt and Cl pseudoorbitals [25] (labeled as BSsp throughout the text). Stabilization energies ΔE^{Stab} were determined as the negative interaction energies between Pt cation and the ligands in the same positions as in the optimized geometry according to the formula:

$$\Delta E^{Stab} = -\left(E_{complex} - \sum E_{ligand} - E_{Pt} \right) \qquad (1)$$

The stabilization energies were corrected for the Basis Set Superposition Error (BSSE) [47–49] and are collected in Table 2 below.

Bonding and association energies were estimated using a following equation:

$$BE = E_{complex} - E_L - E_{CL} \qquad (2)$$

where the E_L is the BSSE corrected energy of the given ligand (computed with the ghost AO functions on the remaining part of the complex) and E_{CL} is the complementary part of the complex treated likewise.

In some cases the global minimum of the reactant/product supermolecule (RxM/PxM where x=1,2) does not correspond to the initial/end state on the reaction coordinate. Therefore, an additional local minimum (Rx/Px) has to be evaluated for such reaction courses in order to obtain correct potential energy surface (PES) for the determination of the rate constants [26]. These constants were estimated using the Eyring's Transition State Theory (TST) according to the formula:

$$k^{TST}(T) = \frac{kT}{h} e^{-\Delta G^{\neq}/kT} \qquad (3)$$

where $\Delta G^{\neq}$ is the Gibbs free energy of the transition state. The electronic structure calculations were performed with the Gaussian03 program package. Program NBO v. 5.0 from Wisconsin University [50] was employed to compute the partial charges using the Natural Bond Orbital (NBO) analysis.

Structural parameters

Usually, reaction coordinates for the hydration process do not contain only one transition state between the global

minima of reactants and products (RxM or PxM) but contain also higher-laying local minima with appropriate orientation of exchanged water and Cl⁻ particles. It is assumed that concentrations of supermolecules corresponding to these minima are in equilibrium with concentrations of the supermolecules corresponding to the global minima over the course of the hydration reactions. All stationary points from reaction coordinate for the two platinum(IV) complexes JM149 and JM216 were optimized at both gas phase and COSMO approximation. The most important structural parameters (distances from central Pt atom) are summarized in Tables 1a and b.

Comparing the Pt-Cl bond length, it can be seen that in all studied complexes they become elongated after solvation. In the TS structures, Hammond's postulate [51] is satisfied, which can be demonstrated on the Pt-Cl and Pt-O bond lengths in comparison with corresponding distances of reactants and products, respectively. The same conclusion also follows from the energy decomposition and/or thermodynamic description of the reactions. An interesting insight into the bonding properties can be obtained from Table 1 comparing the isolated (gas phase) and solvated complexes. It was shown that H-bonding (described either explicitly or by the implicit solvent model) causes elongation of the Pt-Cl bond. On the contrary, if the H-bond concerns proton of the Pt donating ligand (NH_3 or H_2O) the corresponding Pt-N/O bond is shortened.

Another important effect, which has to be taken into account, is the trans-influence. This influence is the highest in the case of hydroxo-ligand, followed by chloro-, CHA-, ammine-, and aqua-ligands. This effect is in the case of the first two ligands enhanced by their negative charge. The higher trans-influence of CHA ligand than ammine explains why the dechloration process in trans position to CHA was assumed to occur in the first hydration step. This influence is also responsible for longer Pt – N_{CHA} distances in the supermolecule representing the reactant of the second hydration step (where hydroxo-ligand is present in trans position) than in the first step where the chloro-ligand is coordinated in both JM149 and JM216 complexes and both considered phases. Similarly the Pt-N_{CHA} bond is shorter in products of the first reaction step where aqua-ligand is in trans position than in both reactants where chloro (and hydroxo) ligands are present.

In the following subsection, structural details of reaction intermediates formed during the hydration of JM149 are described, while the second subsection is devoted to Satraplatin (JM216) and the third subsection to the JM118 complex. In all cases, both hydration steps start with the neutral Pt complex. (In order to keep the total charge constant during the whole two-step process, the aqua-ligand in the product of the first hydration step is replaced by the hydroxo-ligand in a reactant of the second step). This assumption simplifies the comparison of both reaction steps since all the complexes are electroneutral and also better corresponds to real samples [5].

JM149

In the first hydration step of JM149, global (R1M/P1M) and local minima (R1/P1) have to be distinguished in the case of both reactant and product supermolecules. All optimized structures are displayed in Fig. 1. In the supermolecule of the global minimum (R1M), the approaching water is stabilized between NH_3, CHA, and OH ligands. A very short H-bridge of 1.74 Å associates water molecule with hydroxo-ligand (1.66 Å in gas phase). In the local minimum (R1) similar water stabilization exists in the neighboring octant of the octahedral Pt(IV) complex defined by CHA, Cl, and OH ligands. Nevertheless the distance between water and hydroxo ligand is larger (1.98 Å), therefore the additional H-bond interaction is weaker and this arrangement of the supermolecule is less stable. In the TS structure, the 'valence' angle between O-Pt-Cl of the exchanging ligands is 60 deg showing the ligands are quite closely 'packed' around the Pt(IV) cation. The local minimum of the product state (P1) has the released Cl⁻ anion stabilized by protons of aqua and NH3 ligands lying nearly exactly in the O_{aq} – Pt – N_{NH3} plane due to symmetrical repulsion from both hydroxo-ligands (cf. Fig. 1). Passing between product minima, an interesting effect can be noticed when chloride moves from one octant to another, proton from the aqua ligand follows it. This effect can be called "chloride-assisted proton transfer" (ClAPT). This means that different conformers can be formed concerning the arrangement of the hydroxo/aqua ligands. The structure of the global minimum is in this way stabilized by the interaction of the released chloride localized between both amine groups and aqua ligand (by ca 10 kcal mol⁻¹), cf. Fig. 1.

In the 2nd step all five stationary states can be again distinguished as in the previous reaction. The optimized geometries are displayed in Fig. 2. In the global reactant minimum, the approaching water molecule is stabilized between two hydroxo and ammine ligands where the first two H-bond interaction are relatively strong as follows from the corresponding distances in the implicit solvent: 1.76 Å and 2.07 Å, respectively. Local reactant minimum has the water molecule in the vicinity of Cl ligand being replaced so that only one strong H-bond remains between hydroxo ligand (deprotonated aqua ligand introduced in the previous reaction step) and proton of the incoming water: d(O..H)=1.73 Å in the COSMO model. In the TS structure the angle between O-Pt-Cl atoms of exchanging ligands (61 deg) is slightly larger than in TS1. The leaving Cl anion remains in the local minimum H-bonded to aqua and amino groups of CHA ligand with the Cl..H(aq) H-bond equal to 1.96 Å. The best stabilization of chloride particle occurs in neighboring octant after the above-mentioned ClAPT. In this way, Cl⁻ associates to three protons from aqua and both the CHA and ammine groups

Table 1 Structural parameters (Pt-X bond distances) of the Pt complexes from reaction coordinates. a) hydration of JM149 complex both in gas phase and COSMO method), b) JM216 and c) JM118. IC means isolated (not supermolecular) Pt-complex

	Cl_1	Cl_2	N_{NH3}	N_{CHA}	$O_{OH/acet2}$	$O_{OH/acet2}$	O_1	O_2
a)								
IC	2.351	2.342	2.086	2.100	2.020	2.031	–	–
R1M	2.355	2.346	2.087	2.102	2.009	2.049	3.457	–
R1	2.355	2.353	2.088	2.103	2.045	2.012	3.691	–
TS1	3.115	2.345	2.090	2.047	2.044	2.024	2.552	–
P1	4.023	2.353	2.079	2.055	2.014	2.024	2.065	–
P1M	3.758	2.352	2.065	2.025	1.963	2.137	1.993	–
R2M	–	2.352	2.074	2.115	2.043	2.015	2.000	3.488
R2	–	2.352	2.064	2.106	2.018	2.031	2.008	3.665
TS2	–	3.053	2.001	2.117	2.025	2.025	2.000	2.588
P2	–	3.915	2.032	2.116	2.016	2.022	1.994	2.050
P2M	–	3.769	2.103	2.105	1.966	2.122	1.990	1.981
IC s	2.380	2.375	2.060	2.086	2.030	2.034		
R1M	2.383	2.377	2.066	2.089	2.049	2.019	3.539	
R1	2.380	2.376	2.071	2.091	2.020	2.044	3.833	
TS1	2.362	3.299	2.062	2.026	2.019	2.020	2.841	
P1	4.177	2.363	2.067	2.050	2.024	2.022	2.095a	
P1M	3.926	2.367	2.058	2.023	2.135a	1.966	2.001	
R2M		2.372	2.058	2.107	2.018	2.045	2.015	3.533
R2		2.378	2.048	2.103	2.031	2.027	2.018	3.822
TS2		3.171	1.985	2.112	2.028	2.022	2.004	2.745
P2		4.021	2.015	2.117	2.028	2.017	1.998	2.083a
P2M		3.951	2.090	2.108	2.124a	1.968	1.997	1.993
b)								
IC	2.353	2.359	2.087	2.118	2.038	2.045	–	–
R1M	2.363	2.357	2.091	2.120	2.032	2.050	4.232	–
R1	2.369	2.364	2.090	2.105	2.041	2.041	3.889	–
TS1	3.073	2.382	2.079	2.060	2.042	2.041	2.695	–
P1M	4.012	2.365	2.088	2.070	2.041	2.033	2.066	–
R2M	–	2.365	2.080	2.119	2.035	2.044	2.003	3.757
R2	–	2.372	2.067	2.146	2.051	2.035	1.987	3.751
TS2	–	3.183	2.012	2.143	2.041	2.019	1.998	2.693
P2M	–	4.006	2.033	2.135	2.034	2.026	1.995	2.068
IC	2.382	2.383	2.066	2.101	2.043	2.045		
R1M	2.386	2.385	2.073	2.102	2.040	2.047	4.366	
R1	2.389	2.385	2.067	2.101	2.042	2.045	4.034	
TS1	3.170	2.379	2.072	2.054	2.040	2.040	2.848	
P1M	4.163	2.375	2.077	2.061	2.035	2.046	2.093	
R2M		2.384	2.066	2.112	2.039	2.041	2.019	3.806
R2		2.389	2.054	2.128	2.035	2.055	2.005	3.816
TS2		3.277	1.999	2.132	2.025	2.030	2.005	2.825
P2M		4.176	2.025	2.131	2.029	2.033	2.000	2.089
c)								
IC	2.333	2.325	2.117	2.147	–	–	–	–
R1M	2.351	2.337	2.098	2.096			3.694	
TS1	2.766	2.338	2.086	2.077			2.454	
P1M	3.922	2.336	2.091	2.059			2.068	
R2M		2.343	2.092	2.109			1.999	3.536
R2		2.355	2.084	2.123			1.985	3.785

Table 1 (continued)

|	Cl$_1$	Cl$_2$	N$_{NH3}$	N$_{CHA}$	O$_{OH/acet2}$	O$_{OH/acet2}$	O$_1$	O$_2$
TS2		2.793	2.073	2.106			1.995	2.391
P2		3.908	2.047	2.111			1.998	2.064
P2M		4.055	2.111	2.052			2.080	1.991
IC	2.376	2.371	2.068	2.079				
R1M	2.380	2.375	2.068	2.078			3.858	
R1	2.385	2.373	2.070	2.074			3.961	
TS1	2.860	2.367	2.063	2.054			2.527	
P1M	4.172	2.361	2.072	2.046			2.099	
R2M		2.373	2.070	2.087			2.033	3.768
R2		2.383	2.058	2.100			2.021	3.957
TS2		2.873	2.039	2.094			2.094	2.541
P2M		4.061	2.032	2.098			2.015	2.091

lowering the energy of the supermolecule by additional 11 kcal mol^{-1}.

JM216 - Satraplatin

Isolated Satraplatin is stabilized by three intramolecular H-bonds: one between oxygen of the first acetyl ligand and a proton of the NH$_3$ group d=1.85 Å, and other two, which are weaker, between hydrogens of NH$_3$ and CHA ligands and oxygen of the second acetyl (corresponding distances are 2.16 Å and 1.93 Å, respectively). Similarly to JM149 the equatorial plane of N, Pt and Cl atoms is practically exactly planar – deviation in COSMO optimized structure is less than 2 deg (in dihedral angles). Hindered rotation of CHA ligand around the Pt-N$_{CHA}$ axis was explored in order to find some other minima, which could help to stabilize various reactant states. It was found that there is one another structure with both protons of amino group of CHA oriented towards the chloro-ligand but this conformer lies about 3 kcal mol^{-1} higher.

In the case of JM216 both hydration steps display only four supermolecular stationary points. The reason consists in the fact that the reaction coordinate ends directly in global minimum. All the structures obtained for the first reaction step are displayed in Fig. 3 and the platinum coordination distances are collected in Table 1b Global reactant minimum exhibits similar H-bonding like the isolated JM216 complex with the exception of two H-bonds of the second acetyl group. Only the stronger coordination to a proton of the CHA group remains (d=1.94 Å). Instead of the second H-bond, the remote water is associated to both carboxyl and ammine group with distances of 1.96 Å and 1.92 Å, respectively (weak direct H-bond is replaced by two H-bridges involving the remote water). In the reactant local minimum, water is moved to next octant where it can directly interact with a chloro-ligand. This movement is linked with destabilization of the supermolecule by 0.5 kcal mol^{-1}. In TS structure
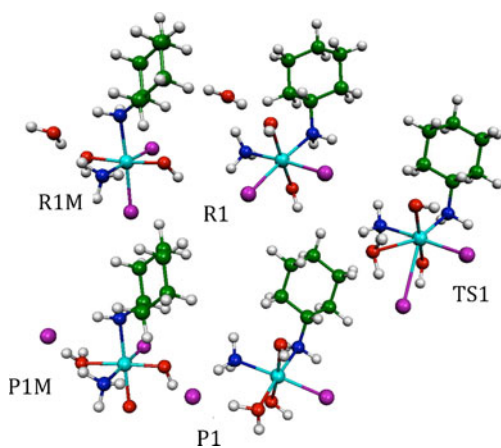
Fig. 1 Structures of stationary points from the reaction energy profile of the first hydration step of the JM149 complex. R1M/P1M labels global reactant/product minimum, R1/P1 – local minima where reaction coordinate starts/ends. Green color is used for C atoms, dark blue for N, red for O, violet for Cl, white for H, and cyan for Pt
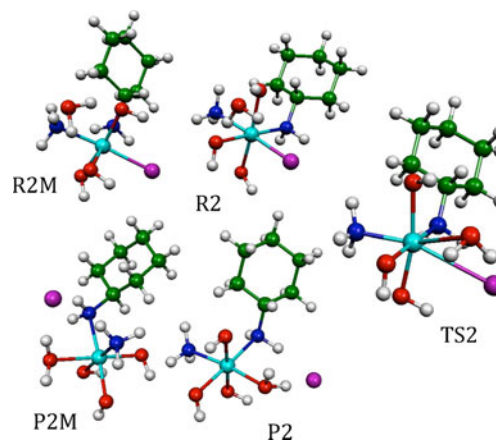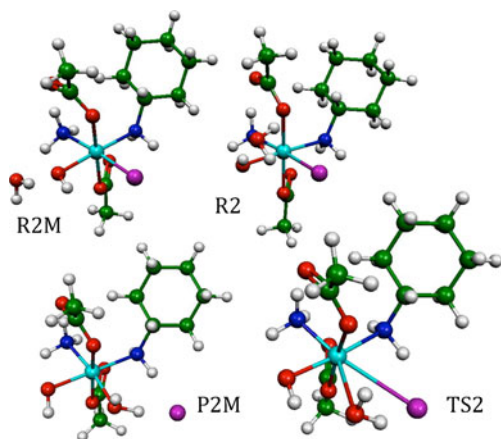

Fig. 2 Structures from the second hydration process JM149
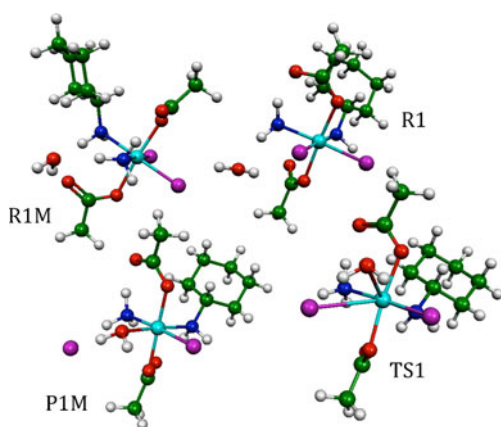
Fig. 3 Supermolecular complexes of JM216 involved in the first hydration

the angle of exchanging ligands (Cl – Pt – O) is 59 deg. This partially corresponds with the fact that acetyl ligands are more bulky than the hydroxo-ligands. The supermolecule is stabilized by several H-bonds: O(acet)…H(CHA) with the distance of 1.87 Å indicating fairly strong interaction and the H-bond between the other acetyl and NH$_3$, (with the distance of 1.89 Å). The only product state has (besides similar acetyl-amino bonding as described above) the remote chloride anion stabilized between the NH$_3$ and aqua ligands where the Cl..H (aq) distance is relatively short (1.92 Å).

The optimal structures of the second hydration step are displayed in Fig. 4. The isolated complex is stabilized via O (acetyl)…H(N) H-bond of 1.86 Å, which is slightly shorter than in the reactant of the first hydration step. While in R2M, the approaching water is stabilized between the NH$_3$, acetyl and OH ligands with strongest interaction to OH group (distance of 1.75 Å), in the local minimum water moves to the vicinity of Cl: octant with OH, Cl, and acetyl ligands where slightly longer water…OH H-bond occurs with the length of about 1.97 Å. In the TS structure, the

angle of Cl–Pt–O is 58 deg, which is the smallest value seen in the Pt(IV) transition states explored. The TS complex is further stabilized by intermolecular H-bonds between the acetyl and NH$_3$ ligand and between the other acetyl and both CHA and NH$_3$ ligands with d(O…H)=1.80 Å, 2.10 Å, and 2.16 Å, respectively. Similar H-bonding pattern can be seen in both explored TS structures lowering (at least partially) the reaction barrier. The final fully hydrated complex has chloride associated with aqua and CHA ligands where all the three intramolecular H-bonds from TS are preserved but (as already mentioned) elongated by ca 0.07 Å.

Pt(II) complex of JM118

The hydrated complex of JM118 is generally accepted as an active form of Satraplatin. Since there are two possible reaction pathways to the final active form, hydration of JM216 followed by reduction of Pt(IV) complex or first reduction to JM118 followed by hydration process, we decided to explore also the hydration reaction of JM118. Coordination parameters (bonds, angles, torsion angles) closely resemble structure of cisplatin. Searching for various minima we rotated the CHA ligand around the Pt-N$_{CHA}$ single-bond. In this way another conformer, analogous to JM216, was found where both protons of nitrogen from CHA interact symmetrically with corresponding chloro-ligand. However, this conformer is ca 9 kcal mol^{-1} higher in energy.

In the global minimum of the reactant of the first hydration step, the water molecule is stabilized between both amino groups by relatively weak H-bonds (distance of oxygen to both NH$_3$ and CHA protons is about 2.01 Å). In the gas phase, a structure of the global minimum is the same as in the reactant minimum of the COSMO approach where instead of two weak H-bonds water remains associated only to NH$_3$ with d (O..H)=1.99 Å, cf. Fig. 5. Since JM118 has the square-planar arrangement, the Cl-Pt-O angle of ligands exchanged in the TS structure is slightly larger (ca 67 deg.). The final product of the first hydration step has the leaving chloride anion localized
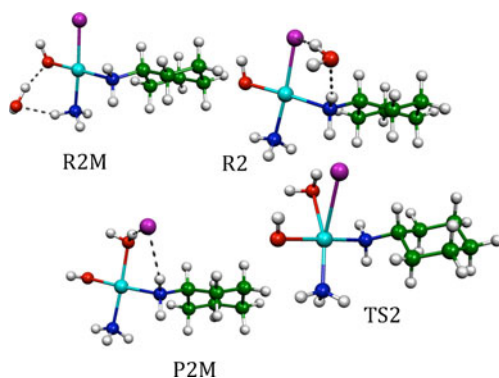

Fig. 4 Structures from the second hydration of JM216
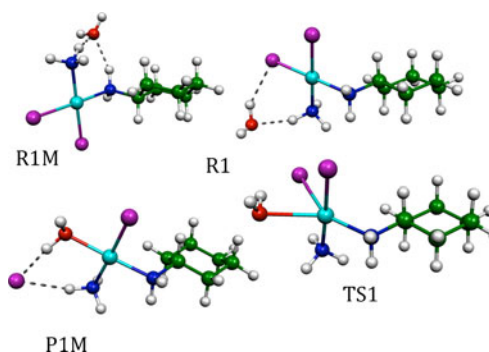
Fig. 5 Hydration of the Pt(II) JM118 complex – geometries of stationary points of the first hydration

between the aqua and NH$_3$ ligands with the stronger association to aqua proton (the Cl..H distance is equal to 2.00 Å).

In the second hydration step, both global and local minima can be distinguished (in the gas phase as well as in the COSMO approach) as can be seen in Fig. 6. Global reactant minimum displays very short H-bond between approaching water and hydroxo-ligand (1.67 Å), which is changed to 2.05 Å in local minimum laying about 4 kcal mol^{-1} higher. The Cl-Pt-O angle is (similarly to first step) about 67 deg. On the contrary to TS1 geometry where the platinum coordination plane was perpendicular to CHA plane, in TS2 the plane is rotated so that hydrogen of Cα carbon in CHA ligands is in cis-orientation to Cl. Global minimum of the product is reached by elongation of Pt-Cl bond and relaxing the final structure. Similarly to JM149 complex, the proton transfer was examined between the aqua and hydroxo ligands in the 2nd hydration step in the COSMO model. Nevertheless, on the contrary to the gas phase, this proton transferred (PT) structure (with aqua ligand in trans position to CHA group) is not lower in energy in the (implicitly) solvated JM118.

Thermochemistry

The energy profile of all reactions was determined in two basis sets as mentioned in the Computational Details. The reaction coordinates using the bigger basis set and the implicit solvent model (the B3LYP/BSsp/COSMO level) are drawn in Fig. 7. The plot is constructed in the way that the energies of second-step reactants are placed to have the same value as the first-step products. Energies of local product minima are not displayed for the sake of clarity. Table 2 collects reaction and activation energies for both optimization and SP basis sets together with enthalpies and Gibbs free energies obtained in both the gas phase and COSMO solvation model. Nuclear degrees of freedom were described by the statistical canonical ensemble of ideal gas for the room temperature (298 K). For a comparison, the
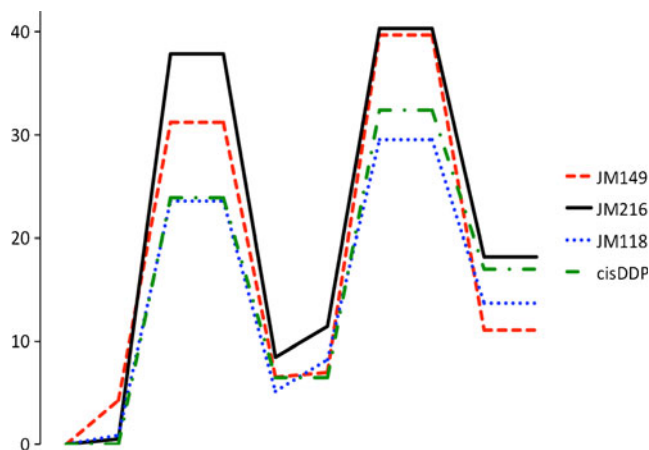
Fig. 7 Gibbs free energy profiles of the hydration reactions of JM149, JM216, JM118, and cisDDP (in kcal mol^{-1}). Energies of the reactants from the second reaction step are placed into the global reaction energies of first-step products and local product stationary points are omitted

hydration energies of cisplatin determined with the same computational setting (in ref. [46]) are also presented.

In accord with the general knowledge of activation of metallodrugs, the hydration is an endothermic/endoergic process, which leads to less stable and thus more reactive products. The driving force for such kind of reactions is low concentration of chloride anions in cellular environment as it is clearly demonstrated in ref. [1].

At the first glance it can be noticed that activation barriers are markedly higher in the case of the Pt(IV) complexes than in the case of Pt(II) ones. The SP values are always over 30 kcal mol^{-1} for the Pt(IV) complexes in both the gas phase and COSMO model. The Pt(II) complexes exhibit substantially lower activation barriers. In the case of JM118, this energy is for both hydration steps about 23–24 kcal mol^{-1}, as can be seen in Fig. 7. The difference between energy barriers of Pt(IV) and Pt(II) complexes represents, according to the TST, decrease of the rate constant by about 5 orders of magnitude at the room temperature.

Binding energies of the ligands and stabilization energies of the isolated complexes

The gas phase binding energies (BEs) of all considered ligands of the isolated complexes JM149, JM216, and JM118 are collected in Table 3. In the last column of Table 3, the gas phase stabilization energies (calculated according to Eq. 1) are presented. All these values are BSSE corrected but do not include the deformation energies. It can be noticed that JM149 is markedly more stable than JM216 (by ca 40 kcal mol^{-1}), which is caused by the interactions between Pt(IV) and the OH group being more pronounced

Fig. 6 Geometries of the second hydration of JM118

Table 2 Reaction energy profile for hydration of JM149, JM216, JM118, and cisplatin (cisDDP) [46] (in kcal mol^{-1})

	$\Delta E_{A(opt)}$	$\Delta E_{R(opt)}$	$\Delta E_{A(SP)}$	$\Delta E_{R(SP)}$	$\Delta H_{(298)}$	$\Delta G_{(298)}$
JM149 - h1_g.p.	47.0	7.5	46.6	7.9	7.7	8.5
JM149 - h2_g.p.	34.2	4.0	35.1	4.8	4.6	5.7
JM149 - h1_COSMO	28.6	5.2	30.0	5.7	5.9	6.5
JM149 - h2_COSMO	32.1	2.6	32.0	3.9	4.1	4.6
JM216 - h1_g.p.	38.0	10.1	39.9	13.0	11.8	13.3
JM216 - h2_g.p.	31.7	11.6	33.7	13.3	12.3	14.3
JM216 - h1_COSMO	32.5	7.1	33.9	8.2	7.9	8.5
JM216 - h2_COSMO	33.9	6.8	32.1	8.4	8.5	9.7
JM118 - h1_g.p.	22.6	2.5	25.9	8.1	7.4	8.6
JM118 - h2_g.p.	26.3	10.7	28.0	14.9	14.1	14.2
JM118 - h1_COSMO	21.8	2.8	23.3	3.8	3.7	5.2
JM118 - h2_COSMO	22.1	10.0	23.7	9.0	8.2	8.5
cisDDP - h1_COSMO	25.0	5.2	25.5	5.9	5.7	6.5
cisDDP - h2_COSMO	27.3	9.1	28.9	12.9	10.8	10.5

than interactions between Pt(IV) and the acetyl group. This correlates quite well with the Pt-O BEs which are by about 20 kcal mol^{-1} smaller in JM216. On the other hand, the H-bonding between acetyl and amino ligands increases the strength of Pt-N bonds in JM216 in comparison to JM149 by ca 5 kcal mol^{-1} for each Pt-N bond. This occurs because when these amino groups donate proton to the N-H…O (acetyl) H-bond some electron density is partially released from the N-H bonding area and can be used for higher donation to the platinum cation. Consequently due to trans-influence, the Pt-Cl bond is slightly weaker by ca 3 kcal mol^{-1} in JM216 than in JM149. Comparing binding energies of Pt(IV) and Pt(II) complexes, all bonds are visibly weaker in JM118. The same conclusion immediately follows also from the comparison of stabilization energies.

substantially reduced (by ca 100 kcal mol^{-1}) due to the effective screening of the electrostatic contribution to these bonds.

Table 4 also demonstrates that the weakest binding occurs in the TS structures. The BEs of forming/breaking Pt-O/Cl bonds in the TS structures are even weaker than BEs of H-bonds which bind the remote particle in the supermolecules representing the global minima of products/reactants. This picture holds also in the gas phase (not shown in Table 4). Therefore, one can say, that neither of these two ligands is really bonded in TS. This can be interpreted so that the dissociative mechanism of the process is the most appropriate. On the other hand, analyzing the vibration modes of the corresponding negative frequencies, the antisymmetric stretch mode of the exchanged ligands was obtained in all explored TS. This leads to the assumption that the reaction rather follows the (pseudo)associative mechanism.

Binding energies of exchanging ligands

In Table 4, the BEs of exchanging ligands in the COSMO model are summarized for all stationary points of the reaction energy profiles of the both hydration steps. Comparing BEs of Pt-Cl bonds of reactants with corresponding gas phase values collected in Table 3, importance of inclusion of the solvent effects is clearly illustrated - all those energies in solution are

Kinetic parameters

Rate constants were computed using TST and are collected in Table 5 for both forward and backward reactions. The rate constants were evaluated at both T=298 K and T=310 K (body temperature). Table 5 clearly demonstrates the importance of the solvent effects, which lead to the substantial

Table 3 Gas phase binding and stabilization energies (in the last column) of isolated JM149, JM216, and JM118 complexes (in kcal mol^{-1})

	Cl_1	Cl_2	N_{NH3}	N_{CHA}	$O_{OH/acet1}$	$O_{OH/acet2}$	Pt
JM149	−159.2	−163.0	−42.4	−49.5	−193.1	−196.8	−2926.4
JM216	−157.7	−159.3	−56.2	−53.4	−172.9	−174.7	−2884.0
JM118	−151.0	−153.9	−38.9	−43.1	−	−	−845.5

Table 4 BSSE corrected Binding Energies (BEs) of exchanged ligand (Cl and H_2O) obtained at the B3LYP/BSsp/COSMO level (in [kcal mol^{-1}])

JM149	Cl	H2O
R1M	−59.3	−11.6
R1	−57.4	−3.3
TS1	−16.0	−8.6
P1	−22.0	−41.2
P1M	−26.5	−36.9
R2M	−60.3	−11.6
R2	−57.5	−8.1
TS2	−23.1	−6.4
P2	−23.1	−41.6
P2M	−24.5	−37.5
JM216		
R1M	−58.5	−6.2
R1	−64.6	−2.9
TS1	−21.1	−3.4
P1M	−24.3	−45.2
R2M	−60.5	−8.1
R2	−58.9	−4.0
TS2	−23.1	−7.0
P2M	−23.4	−45.4
JM118		
R1M	−47.0	−7.4
R1	−53.0	−4.9
TS1	−16.4	−3.7
P1M	−18.5	−41.3
R2M	−50.7	−10.5
R2	−55.5	−4.5
TS2	−16.2	−4.3
P2M	−17.0	−39.9

Table 5 Rate constants for hydration process of JM149, JM216, and JM118 in gas phase and COSMO at the B3LYP/BSsp level

		$k_{fw(298)}$	$k_{rw(298)}$	$k_{fw(310)}$	$k_{rw(310)}$
JM149	h1 g.p.	1.14E-22	1.20E-10	2.27E-21	8.34E-10
	h2 g.p.	6.66E-15	3.58E-06	6.35E-14	1.80E-05
	h1 COSMO	8.15E-11	3.51E-09	6.35E-10	2.37E-08
	h2 COSMO	2.97E-12	3.07E-09	2.63E-11	2.08E-08
JM216	h1 g.p.	2.66E-17	1.30E-07	3.38E-16	7.76E-07
	h2 g.p.	3.24E-13	1.85E-06	2.75E-12	1.00E-05
	h1 COSMO	1.08E-15	4.42E-09	1.29E-14	2.95E-08
	h2 COSMO	2.75E-11	4.53E-07	2.23E-10	2.54E-06
JM118	h1 g.p.	3.89E-07	7.43E-01	2.19E-06	2.41E+00
	h2 g.p.	5.83E-09	9.51E+00	3.86E-08	2.80E+01
	h1 COSMO	3.31E-05	4.56E-02	1.57E-04	1.64E-01
	h2 COSMO	7.99E-06	4.44E+00	4.01E-05	1.35E+01
cisDDP	h1 COSMO	1.91E-05	4.50E+00	9.25E-05	1.36E+01
	h2 COSMO	6.94E-07	3.31E+01	3.83E-06	9.27E+01

decrease of the energy barriers. Comparing the rate constants of JM118 with cisplatin [46] large similarity can be noticed.

The main goal of this study is to compare rate constants for hydration process between the Pt(IV) complexes considering Satraplatin and JM149, and the Pt(II) complexes represented by JM118 (metabolite of Satraplatin) and cisplatin. From Table 5 it is clear that all rate constants of the regarded Pt(IV) complexes are much smaller than the corresponding constants of the Pt(II) complexes. The rate constants of both JM216 and JM149 show that the reaction occurs in time scale of thousands of years, i.e. the hydration process of these complexes is kinetically forbidden reaction. Therefore, we propose that JM216 and JM149 have to be reduced first and only after that the hydration reaction of the Pt(II) complexes may occur.

Partial charge analyses

Natural population analyses (NPAs) were performed for the studied complexes (including both isolated and supermolecular complexes). The partial charges determined by the NPA at the B3LYP/BSsp level with the COSMO model are collected Table 6. Clearly, higher oxidation state of platinum atom correlates with higher Pt partial charge. Also, higher donation of the chloro ligand (less negative partial charge) can be noticed in the case of Pt(IV) complexes in comparison with Pt(II) ones (ca −0.5 vs. -0.6e), which is a consequence of the higher electrostatic contribution from the more positively charged Pt atom in Pt(IV) complexes. Lower donation of CHA group in the product of the first hydration step of JM149 is connected with the fact that PT occurred from the aqua ligand in trans position to the axial hydroxo-group and therefore more pronounced (and more competitive) coordination occurs. The same concerns also the second hydration step where the most stable P2M conformer has aqua ligand in axial position. In this way also lower donation of NH_3 ligand is visible in the P2M structure. From this point of view, a different picture follows from Table 6 for the JM216 hydration where no PT can occur and therefore more pronounced coordination (indicated through less negative partial charge) of nitrogen of the corresponding amino ligands is visible. This is in accord with lower dative ability of water in comparison with amino group (on the contrary to hydroxo ligand). Similarly, stronger donation from nitrogen atom can be also seen in the JM118 complex. Changes of the Pt partial charge of the complexes along the reaction coordinate nicely correspond to lower total donation in TS structures as well as in products comparing with reactants and consequently they are also in accord with lower stability of hydrated complexes (comparing with the original chlorinated analogues). Usually some changes in partial charges of the ligands in cis-positions to exchanged chloro/aqua ligands or in axial positions are caused by

Table 6 NPA partial charges at the B3LYP/BSsp COSMO level with the cavity constructed using the Klamt's atomic radii

		Pt	Cl$_1$	Cl$_2$	N$_{NH3}$	N$_{CHA}$	O$_{axial1}$	O$_{axial2}$	O$_1$	O$_2$
	R1M	1.256	−0.500	−0.508	−0.886	−0.714	−1.029	−0.988	−1.021	
	TS1	1.365	−0.861	−0.488	−0.904	−0.585	−1.012	−1.021	−0.990	
JM149	P1M	1.369	−0.864	−0.504	−0.895	−0.762	−0.897	−0.889	−0.979	
	R2M	1.378	−	−0.523	−0.884	−0.726	−1.006	−1.018	−0.997	−1.027
	TS2	1.500	−	−0.843	−0.763	−0.760	−1.041	−1.015	−0.988	−0.983
	P2M	1.487	−	−0.875	−0.930	−0.752	−0.893	−0.914	−0.995	−0.985
	R1M	1.258	−0.487	−0.478	−0.920	−0.728	−0.688	−0.682	−0.979	
	TS1	1.364	−0.791	−0.479	−0.925	−0.623	−0.686	−0.741	−0.959	
JM216	P1M	1.371	−0.827	−0.468	−0.937	−0.686	−0.680	−0.710	−0.881	
	R2M	1.386		−0.507	−0.912	−0.742	−0.686	−0.694	−0.980	−1.008
	TS2	1.501		−0.818	−0.776	−0.795	−0.682	−0.711	−0.974	−0.981
	P2M	1.492		−0.837	−0.854	−0.786	−0.700	−0.710	−0.960	−0.883
	R1M	0.559	−0.618	−0.616	−0.938	−0.754			−0.982	
	TS1	0.717	−0.848	−0.612	−0.933	−0.714			−0.963	
JM118	P1M	0.669	−0.876	−0.604	−0.957	−0.712			−0.910	
	R2M	0.658		−0.631	−0.945	−0.747			−1.077	−1.025
	TS2	0.812		−0.858	−0.903	−0.766			−1.091	−0.971
	P2M	0.746		−0.894	−0.903	−0.780			−1.086	−0.908

formation of H-bonds (in magnitude up to 0.4 e), which can mask the general trends.

Conclusions

The hydration reactions of the platinum complexes JM149, JM216 and JM118 were explored in this study. The reaction energy profile was determined at the B3LYP/BSsp//B3LYP/BSop level with the COSMO implicit solvation model to describe effects of aqueous solution. The cavities used in the model were constructed using the Klamt's atomic radii. Computed rate constants and activation barriers of the hydration reactions were compared to those of cisplatin, which were explored in our previous study [46].

In the both Pt (IV) complexes JM149 and JM216, the first leaving chloro-ligand is in the trans position to CHA, which has slightly stronger dative ability than NH$_3$ group. The same also holds for the JM118 complex. In the case products of the hydration of JM149, the chloride-assisted proton transfer was observed, which means that when chloride passed from one octant of the octahedral complex to the other, proton follows this movement changing a hydroxo ligand into an aqua ligand. With a few exceptions, structures of global minima of reactants and products do not correspond to minima from which the reaction coordinate starts or ends (IRC minima). These local minima, which are (from definition) higher in energy, have the remote particle H-bonded directly to the other exchanging ligand.

Evaluating the thermodynamics of the hydration reaction, it was confirmed than the hydration process is endothermic/endoergic. Endothermicity is always reduced under 10 kcal mol^{-1} when the solution is considered.

It was verified that the stabilization of Pt(IV) complexes is substantially higher than in the case of Pt(II) complexes.

Based on the analysis of the negative frequencies of TS structures it can be assumed that the hydration process proceeds by the (pseudo)associative mechanism.

It was found that the hydration process of Pt(IV) complexes is substantially slower ($k \approx 10^{-11}$ s^{-1} at T=298 K) than the hydration of the corresponding Pt(II) analogues. Rate constants of the Pt(II) complex JM118 were estimated to be ca 10^{-5} s^{-1}. This suggests that while the hydration process of considered Pt(IV) complexes is kinetically forbidden reaction, the hydration of JM118 may occur at physiological conditions. Comparison with the data for cisplatin, which were published recently [1, 46], confirms the close physico-chemical relationship of JM118 and cisplatin.

References

1. Zimmermann T, Leszczynski J, Burda JV (2011) J Mol Model 17:2385–2393

2. Alderden RA, Hall MD, Hambley TW (2006) J Chem Educ 83:728–724
3. Wheate NJ, Walker S, Craig GE, Oun R (2010) Dalton Trans 39:8113–8127
4. Ehrsson H, Wallin I, Yachnin J (2002) Med Oncol 19:261–265
5. Lippert B (ed) (1999) Cisplatin: chemistry and biochemistry of a leading anticancer drug. Wiley-VCH Verlag GmbH, Wienheim, 1999
6. Kasparkova J, Marini V, Najajreh Y, Gibson D, Brabec V (2003) Biochem 42:6321–6332
7. Bloemink MJ, Heetebrij RJ, Ireland J, Deacon GB, Reedijk J (1996) J Biol Inorg Chem 1:278–283
8. Farrell N, Kelland LR, Roberts JD, Van Beusichem M (1992) Cancer Res 52:5065–5072
9. Kasparkova J, Novakova O, Farrell N, Brabec V (2003) Biochemistry 42:792–800
10. Deubel DV (2006) J Am Chem Soc 128:1654–1663
11. Lau JKC, Deubel DV (2006) J Chem Theory Comput 2:103–106
12. Chval Z, Šíp M (2000) J Mol Struct (THEOCHEM) 532:59–68
13. Chval Z, Sip M, Burda JV (2008) J Comput Chem 29:2370–2381
14. Raber J, Zhu C, Eriksson LA (2005) J Phys Chem 109:11006–11015
15. Zhu C, Raber J, Eriksson LA (2005) J Phys Chem B 109:12195–12205
16. Costa LA, Hambley TW, Rocha WR, Almeida WB, Dos Santos HF (2006) Int J Quantum Chem 106:2129–2144
17. Costa LAS, Rocha WR, De Almeida WB, Dos Santos HF (2003) J Chem Phys 118:10584–10592
18. Costa LAS, Rocha WR, De Almeida WB, Dos Santos HF (2005) J Inorg Biochem 99:575–583
19. Dos Santos HF, Marcial BL, De Miranda CF, Costa LAS, De Almeida WB (2006) J Inorg Biochem 100:1594–1605
20. Lopes JF, Menezes VSD, Duarte HA, Rocha WR, De Almeida WB, Dos Santos HF (2006) J Phys Chem B 110:12047–12054
21. Lopes JF, Rocha WR, Dos Santos HF, De Almeida WB (2008) J Chem Phys 128:165103
22. Lopes JF, Rocha WR, dos Santos HF, de Almeida WB (2010) J Braz Chem Soc 21:887–896
23. Carloni P, Sprik M, Andreoni W (2000) J Phys Chem B 104:823–835
24. Spiegel K, Rothlisberger U, Carloni P (2004) J Phys Chem B 108:2699–2707
25. Burda JV, Zeizinger M, Šponer J, Leszczynski J (2000) J Chem Phys 113:2224–2232
26. Burda JV, Zeizinger M, Leszczynski J (2005) J Comput Chem 26:907–914
27. Burda JV, Šponer J, Hrabáková J, Zeizinger M, Leszczynski J (2003) J Phys Chem B 107:5349–5356
28. Burda JV, Šponer J, Leszczynski J (2000) J Biol Inorg Chem 5:178–188
29. Burda JV, Leszczynski J (2003) Inorg Chem 42:7162–7172
30. Zeizinger M, Burda JV, Leszczynski J (2004) Phys Chem Chem Phys 6:3585–3590
31. Zimmermann T, Zeizinger M, Burda JV (2005) J Inorg Biochem 99:2184–2196
32. Zimmermann T, Burda JV (2009) J Chem Phys 131:135101
33. Zimmermann T, Burda JV (2010) Dalton Trans 39:1295–1301
34. Fokkema E, Groen HJM, Helder MN, de Vries EGE, Meijer C (2002) Biochem Pharmacol 63:1989–1996
35. Galettis P, Carr JL, Paxton JW, McKeage MJ (1999) J Anal At Spectrom 14:953–956
36. Kelland LR, Abel G, McKeage MJ, Jones M, Goddard PM, Valenti M, Murrer BA, Harrap KR (1993) Cancer Res 53:2581–2586
37. Goddard PM, Orr RM, Valenti MR, Barnard CF, Murrer BA, Kelland LR, Harrap KR (1996) Anticancer Res 16:33–38
38. Poon GK, Mistry P, Raynaud FI, Harrap KR, Murrer BA, Barnard CFJ (1995) J Pharm Biomed Anal 13:1493–1498
39. Kelland LR, Sharp SY, O'Neill CF, Raynaud FI, Beale PJ, Judson IR (1999) J Inorg Biochem 77:111–115
40. Raynaud FI, Mistry P, Donaghue A, Poon GK, Kelland LR, Barnard CFJ, Murrer BA, Harrap KR (1996) Cancer Chemother Pharmacol 38:155–162
41. Farrell N, Povirk LF, Dange Y, DeMasters G, Gupta MS, Kohlhagen G, Khan QA, Pommier Y, Gewirtz DA (2004) Biochem Pharmacol 68:857–866
42. Andzelm J, Kolmel C, Klamt A (1995) J Chem Phys 103:9312–9320
43. Klamt A, Schuurmann G (1993) J Chem Soc Perkin Trans:2799–805.
44. Andrae D, Haussermann U, Dolg M, Stoll H, Preuss H (1990) Theor Chim Acta 77:123–141
45. Bergner A, Dolg M, Kuechle W, Stoll H, Preuss H (1993) Mol Phys 80:1431–1439
46. Chval Z, Futera Z, Burda JV (2011) J Chem Phys 134:024520
47. Boys SF, Bernardi F (1970) Mol Phys 19:553–566
48. Urban M, Hobza P (1975) Theor Chim Acta 36:207–214
49. Urban M, Hobza P (1975) Theor Chim Acta 36:215–220
50. Weinhold F (2001) NBO 5.0 Program University of Wisconsin, Madison, Wisconsin 53706, Wisconsin.
51. Hammond GS (1955) J Am Chem Soc 77:334–338